ChemPubSoc Europe
DOI: 10.1002/chem.201803506
CHEMISTRY A European Journal Full Paper

Organocatalysis

Direct Enantio- and Diastereoselective Oxidative Homocoupling of Aldehydes

Line Næsborg, Lars A. Leth, Gabriel J. Reyes-Rodríguez, Teresa A. Palazzo, Vasco Corti, and Karl Anker Jørgensen*[a]

Abstract: A novel strategy for the direct enantioselective oxidative homocoupling of α-branched aldehydes is presented. The methodology employs open-shell intermediates for the construction of chiral 1,4-dialdehydes by forming a carbon–carbon bond connecting two quaternary stereogenic centers in good yields and excellent stereoselectivities for electron-rich aromatic aldehydes. The 1,4-dialdehydes were transformed into synthetically valuable chiral pyrrolidines. Experimental mechanistic investigations based on competition experiments combined with computational studies indicate that the reaction proceeds through a radical cation intermediate and that reactivity and stereoselectivity follow different trends.

Introduction

The direct stereoselective α-coupling of two carbonyl moieties into chiral 1,4-dicarbonyl compounds is a challenge due to the dual nucleophilicity of the reacting species and, to the best of our knowledge, has not yet been achieved. Indirect carbon–carbon couplings have traditionally been performed by oxidation of pre-formed enolates.[1] This elegant approach has been pursued by Baran and co-workers in the coupling of, for example, oxazolidinones and oxindoles with ketones applying lithium diisopropylamide (LDA) with copper(II) or iron(III).[2] Furthermore, Robinson and Thomson disclosed a related oxidative coupling of cyclic ketones by silyl-bis-enol ethers.[3] These reactions generated racemic products with low diastereoselectivities and moderate yields. To further investigate these reactions, Casey and Flowers applied ^{7}Li NMR to elucidate the mechanism for the oxidative coupling of lithium enolates.[4] Finally, Hirao and co-workers demonstrated that oxo-vanadium(V) induces coupling between boron and silyl enolates.[5]

Aldehydes are a cornerstone of organocatalysis and have been applied in HOMO and LUMO tuning strategies and extended to SOMO activation through single-electron transfer (SET) using various oxidants.[6] In particular, MacMillan and co-workers reported an oxidative α-coupling of aldehydes between an enamine-based radical cation and a pre-formed silyl-enol ether (Scheme 1 a).[7]

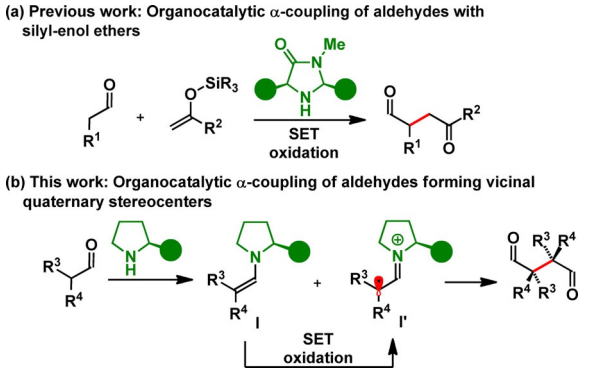

Scheme 1. (a) Organocatalytic α-coupling of aldehydes with silyl-enol ethers; (b) direct organocatalytic α-coupling of aldehydes mediating the construction of vicinal quaternary stereogenic centers.

An important aspect of the α-coupling of aldehydes is the potential for stereoselective construction of vicinal quaternary carbons. Strategies for the stereoselective generation of such carbon–carbon bonds are underdeveloped. According to the literature, there are a variety of reasons for this, including steric repulsion and the difficulties in selectively activating coupling partners.[2] We envisioned a concept based on the direct coupling of α-branched aldehydes for the stereoselective construction of vicinal quaternary stereocenters in succinic 1,4-dialdehydes. An open-shell species of a catalytically generated enamine intermediate was anticipated to overcome the immense energetic barrier required to form the bond connecting two quaternary stereogenic centers.[8] Here, we disclose the first oxidative organocatalytic strategy for the diastereo- and enantioselective coupling of α-branched aldehydes (Scheme 1 b).

The oxidative organocatalytic concept relies on an aldehyde condensing with an aminocatalyst to form enamine **I**, which is oxidized to generate the radical cation **I′**. Intermediate **I′** is proposed to react stereoselectively with the enamine-nucleophile

[a] L. Næsborg, L. A. Leth, Dr. G. J. Reyes-Rodríguez, Dr. T. A. Palazzo, V. Corti, Prof. K. A. Jørgensen
Department of Chemistry
Aarhus University
8000 Aarhus (Denmark)
E-mail: kaj@chem.au.dk

Supporting information, including experimental and computational details as well as crystallographic data, and the ORCID number(s) for the author(s) of this article can be found under https://doi.org/10.1002/chem.201803506.

I to construct a carbon–carbon bond (Scheme 1 b). In the following discussion, we present the development and scope of the catalytic α-coupling of α-branched aldehydes affording enantioenriched 1,4-dialdehydes with vicinal quaternary carbons, and their transformation into synthetically valuable chiral pyrrolidines. Mechanistic investigations through competition experiments and computational studies were carried out to obtain information about the reactivity and selectivity of the presented methodology.

Results and Discussion

Recently, we reported that α,β-unsaturated aldehydes undergo stereoselective γ-couplings in the presence of Cu^{II}, an aminocatalyst, and air (O_2) as terminal oxidant.[9] When testing linear aldehydes under these conditions, a product containing a carbon-carbon double bond connecting the two aldehydes was obtained. A similar result has previously been reported for ketones.[10] Encouraged by the observed reactivity, we envisioned that α-branched aldehydes might circumvent double-bond formation, allowing for the formation of vicinal quaternary carbons in a stereoselective manner. Subjecting 2-(6-methoxynaphthalen-2-yl)propanal **1 a** to air/Cu^{II}[9] provided 1-(6-methoxynaphthalen-2-yl)ethan-1-one as an oxidative byproduct (Table 1, entry 1). To avoid this undesired reaction, a search for different conditions was initiated applying Ag_2CO_3 as the oxidant with various aminocatalysts (entries 2–4). Employing Ag_2CO_3 increased conversion to 1,4-dialdehyde **3 a**, and catalyst **2** led to superior yields and stereoselectivities. A short screening of metal salts revealed that Ag_2CO_3 was the optimal oxidant (entries 5, 6). Introduction of 4-NO_2-$PhCO_2H$ (150 mol%) led to a dramatic increase of yield and stereoselectivity (entry 7). Lower loadings of 4-NO_2-$PhCO_2H$ led to an increased amount of the oxidative byproduct 1-(6-methoxynaphthalen-2-yl)ethan-1-one. Control experiments in the absence of aminocatalyst or Ag_2CO_3 displayed no reactivity (entries 8, 9). This screening revealed that Ag_2CO_3 displayed the best oxidative properties and, in combination with aminocatalyst **2** (20 mol% per equiv of **1 a**), afforded **3 a** in the presence of 4-NO_2-$PhCO_2H$ in CH_2Cl_2. These optimized reaction conditions were used to investigate a representative scope of the enantioselective homocoupling of α-branched aldehydes (Table 2).

Table 2 demonstrates that the stereoselective α-coupling of electron-rich aromatic aldehydes proceeds smoothly. Reaction of an aldehyde bearing a methoxy-naphthyl moiety (**1 a**) provided **3 a** in 78% yield and excellent stereoselectivity (92% *ee*, 12:1 d.r.). It should be noted that the minor diastereoisomer is the *meso*-product. Comparable results were obtained for the naphthyl-substituted aldehyde **1 b**. Aldehydes with methoxyphenyl substituents (**1 c**,**d**) provided the α-coupled products **3 c**,**d** in similar yields and stereoselectivities. We were pleased to observe that **3 e** was obtained in 75% yield, 94% *ee*, and 5:1 d.r. despite possible incompatibilities of the thioether due to potential oxidation events.[11] Furthermore, the reaction of 2-(*p*-tolyl)propanal **1 f** afforded **3 f** in 63% yield, 94% *ee*, and 5:1 d.r. The results in entries **3 g**–**i** reflect that electron-poor aromatic aldehydes are less suited for this oxidative homocoupling because they display lower yields and stereoselectivities. To demonstrate the synthetic potential of the 1,4-dialdehydes **3** obtained from this stereoselective coupling, reduc-

Table 1. Screening results for the oxidative homocoupling of α-branched aldehyde **1 a**.[a]

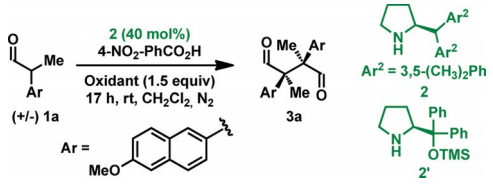

Entry	4-Nitrobenzoic acid [mol%]	Oxidant	Conversion [%]	d.r.	*ee* [%]
1[b,c]	0	$Cu(OAc)_2$/air	4	1:1	–
2[c]	0	Ag_2CO_3	90	1:1	46
3[d]	0	Ag_2CO_3	89	1:1	0
4	0	Ag_2CO_3	96	2:1	60
5	0	$AgNO_3$[e]	27	2:1	>99
6	0	$FeCl_3$[e]	0	–	–
7[f]	150	Ag_2CO_3	>95 (78)	7:1	92
8[g]	150	Ag_2CO_3	0	–	–
9	150	–	0	–	–

[a] Reactions were carried out on a 0.05 mmol scale with 2.0 equiv of **1 a** and 40 mol% of the aminocatalyst **2** (it should be noted that this corresponds to 20 mol% per equiv of aldehyde) in 0.4 mL of solvent. Conversion was determined by ^{1}H NMR analysis. Isolated yield is given in parentheses. Diastereomeric ratios were calculated from ^{1}H NMR spectra of the crude products. [b] 20 mol% $Cu(OAc)_2$ was employed in an open-air system. [c] The catalyst **2′** was employed. [d] L-Proline was employed as catalyst. [e] 3 equiv of metal salt used. [f] Reactions were carried out on a 0.1 mmol scale. [g] Control experiment performed in the absence of organocatalyst.

Table 2. Organocatalytic enantioselective oxidative homocoupling of α-branched aldehydes.[a]

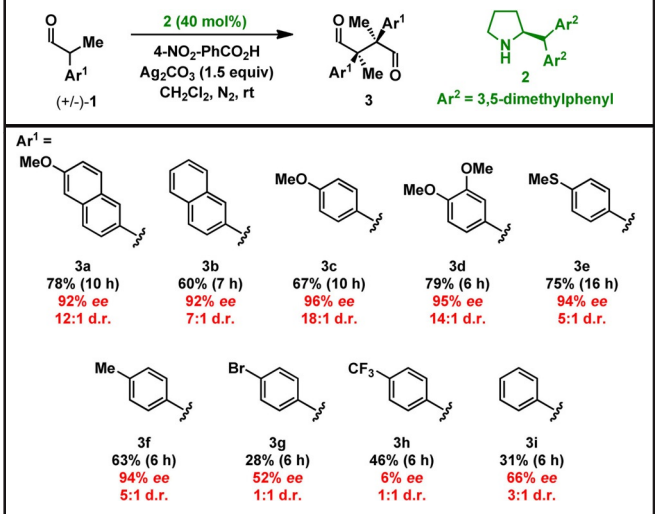

[a] Reactions were performed on a 0.1 mmol scale. Diastereomeric ratio (d.r.) determined by ^{1}H NMR after flash column chromatography. Enantiomeric excess (*ee*) determined by a chiral stationary phase UPC^2. Absolute stereochemistry determined by analogy to single-crystal X-ray crystallographic analysis of **4 c·HBr** (vide infra).

Table 3. Reductive amination of homo-coupling products **3a–c** for the formation of chiral pyrrolidines **4a–c**.[a]

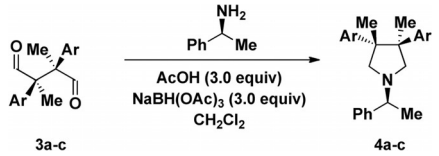

Ar =

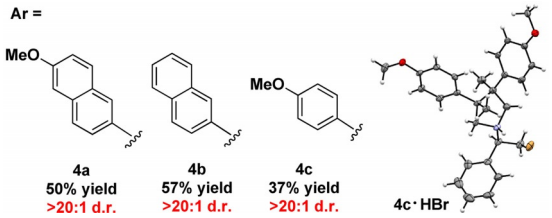

4a	4b	4c	4c·HBr
50% yield	57% yield	37% yield	
>20:1 d.r.	>20:1 d.r.	>20:1 d.r.	

[a] Reactions were performed on a 0.1–0.14 mmol scale; d.r. determined by ^{1}H NMR after flash column chromatography.

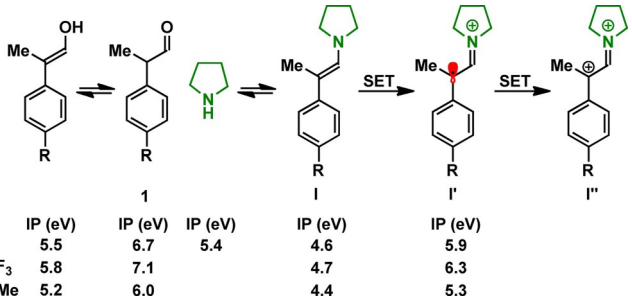

R:	IP (eV)	IP (eV)	IP (eV)	IP (eV)	IP (eV)
H	5.5	6.7	5.4	4.6	5.9
CF_3	5.8	7.1		4.7	6.3
OMe	5.2	6.0		4.4	5.3

Scheme 2. Calculated IPs of α-branched aldehydes, truncated organocatalyst **2** (pyrrolidine), and intermediates.

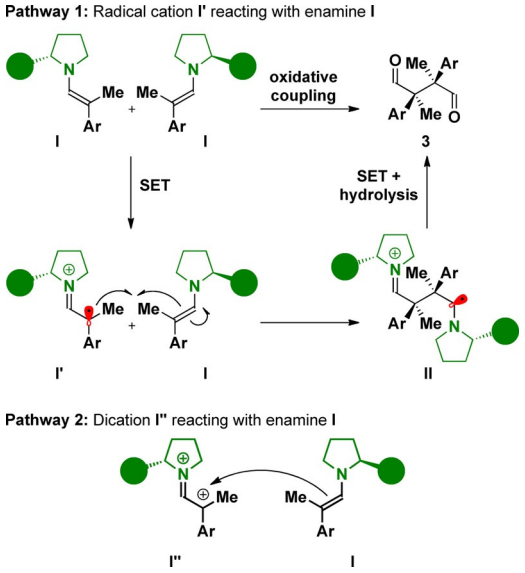

Scheme 3. Proposed reaction mechanism (pathway 1) and another conceivable reaction pathway for the oxidative homocoupling of α-branched aldehydes (pathway 2).

tive aminations of **3a–c** were performed (Table 3). Reaction of **3a-c** with (*S*)-1-phenylethan-1-amine provided the corresponding pyrrolidines **4a–c**. This class of interesting pyrrolidine core structures has been applied as ligands and catalysts in methodology development.[12] Additionally, pyrrolidines are privileged heterocycles in bioactive molecules.[13]

The present reaction concept enables unprecedented enantioselective coupling of α-branched aldehydes. This methodology overcomes the difficulties in connecting two quaternary stereogenic carbons and affords the homocoupled products in good yields and high stereoselectivities for electron-rich aldehydes. Encouraged by these results, we sought to obtain insight into the reaction mechanism to understand the factors that govern reactivity. Density functional theory (DFT) was used to determine the ionization potentials (IPs) of all relevant species (Scheme 2). The calculations support a chemoselective pathway by revealing enamine **I** to be more susceptible to oxidation than the α-branched aldehydes, enols, or organocatalyst, in accordance with prior results.[6c,14] Oxidation of **I′** to a dicationic system **I″** is calculated to be higher in energy. The IPs (Scheme 2) reflect the energy required to remove one electron from the corresponding species. The IP values for oxidizing **I′** to **I″** are additive (e.g., oxidation of **I** bearing a hydrogen to **I″** requires 10.5 eV).

Two conceivable reaction pathways for this oxidative coupling of α-branched aldehydes are considered; 1) radical cation **I′** reacting with neutral enamine **I**, and 2) dication **I″** reacting with neutral enamine **I**. IPs and observed reactivity could support the mechanism proposed in pathway 1 (Scheme 3). It relies on the assumption that two equivalents of enamine **I** are formed by the reaction of the α-branched aldehyde with organocatalyst **2**. One of the formed intermediates undergoes SET oxidation by Ag^I generating radical cation **I′**. This intermediate is envisioned to react with enamine **I** providing adduct **II**, from which the 1,4-dialdehyde **3** is formed by subsequent SET oxidation by Ag^I and hydrolysis. It is also possible that an enol species reacts with an oxidized enamine **I′**. Additionally, we cannot rule out radical recombination in this mechanism, though the reaction times and product distributions might suggest radical recombination to be unlikely (see the Supporting Information).

The following sections describe the experiments performed to obtain information discerning these two conceivable pathways, and to provide insight into this oxidative homocoupling. We set out to gain additional evidence for the proposed pathway proceeding through radical cation **I′** rather than dication **I″** (i.e., differentiating pathways 1 and 2). A Newcomb radical-clock experiment could distinguish between these intermediates,[15] however, no radical adducts were observed. Traditional kinetic methods could be employed to distinguish these pathways, but unfortunately, they were not suitable due to the heterogeneity of the reaction mixture.[16] Competition experiments proved effective as a means of evaluating linear free energy relationships to discern the nature of the oxidized enamine intermediate.

We measured relative rates of the oxidative coupling in binary mixtures of *para*-substituted 2-phenyl propanals **1** by carrying out separate experiments under the same reaction conditions. These were measured by a competitive method based on product ratios and determined by ^{1}H NMR.[17–19] Rela-

tive reactivities can provide valid rate measurements given that the reaction being analyzed is under kinetic control and that the competing processes are of the same kinetic order.[18,19] It should be noted that the coupling of **I** and **I′** (Scheme 3) is not proposed to be rate-determining, but product-determining. The rate-determining step is likely the SET oxidation generating **I′**, which is affected not only by the electronics of the substrate (as in the case of the calculated IPs, Scheme 2), but also by the insolubility of the oxidant.[16]

Product ratios from the competition experiments and full details regarding relative rate determination by direct and indirect methods can be found in the Supporting Information. The following general trend is observed: enamines having more radical-stabilizing substituents undergo faster oxidative couplings compared to their less-stabilized counterparts. For example, the *para*-methoxy-substituted enamine reacts 4.7 times as fast as the unsubstituted species (Table 4, line 1). Despite the disparity in the rate- and product-determining steps, this trend is reflected by the calculated enamine IPs (**I**→**I′**, Scheme 2), in which IP(OMe) < IP(H) < IP(CF_3).

The relative reactivities presented in red in Table 4 enable a Hammett analysis allowing for more specific information regarding which of the two intermediates (**I′** or **I″**) is involved.[18] Figure 1 shows four Hammett-type plots for the oxidative coupling of *para*-substituted 2-phenyl propanals **1**. Figure 1 a shows poor linear correlation between log($k_{R\text{-}Ph}/k_{Ph}$) and the substituent parameter σ^+ ($R^2 = 0.46$).[20] Gratifyingly, a linear correlation between log($k_{R\text{-}Ph}/k_{Ph}$) and the substituent parameter $\sigma^\bullet$ was obtained ($R^2 = 0.98$, Figure 1 b).[21] This supports that radical cation **I′** is the reactive species, rather than dication **I″** and distinguishes pathways 1 and 2 (Scheme 3). In addition, the plot in Figure 1 b has a value of $\rho = 2.8$ suggesting that the reactive intermediate **I′** is highly sensitive to substituents.[18] Despite the compatibility of thioether **1 e** for the synthetic approach, it is excluded from the linear fit because the sulfur could be prone to participate in other oxidation events.[11] This is supported by spin-density calculations in which a large radical contribution was observed at the sulfur atom in comparison to other substrates (see the Supporting Information).

Table 4. Relative reactivities of enamines $k_{R\text{-}Ph}/k_{R\text{-}Ph}$ in oxidative couplings. The values presented in italics are averages of four indirect measurements.

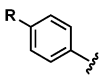

R =	MeO 3c	MeS 3e	Me 3f	Br 3g	F_3C 3h	H 3i
R	MeS	Me	Br	F_3C	H	
MeO	1.2 *1.0 ± 0.1*	3.1 *2.4 ± 0.8*	2.6 *3.0 ± 0.8*	2.7 *3.4 ± 0.9*	4.7 *6 ± 1*	
MeS	1	3.0 *2.1 ± 0.3*	2.6 *2.8 ± 0.8*	3.0 *3 ± 1*	4.4 *5 ± 1*	
Me	–	–	1.3 *1.1 ± 0.3*	1.5 *1.1 ± 0.2*	2.3 *2.1 ± 0.7*	
Br	–	–	1	1.0 *1.1 ± 0.1*	2.1 *1.9 ± 0.4*	
F_3C	–	–	–	1	1.7 *1.7 ± 0.3*	

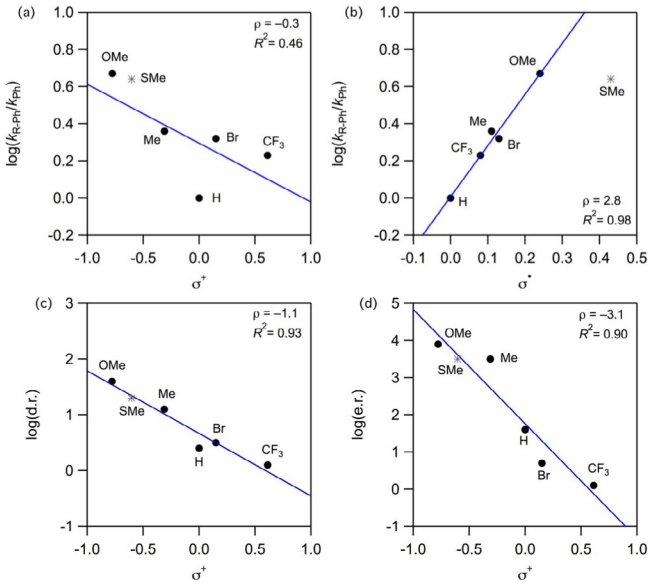

Figure 1. Hammett-type plots for *para*-substituted 2-phenyl propanals. (a) log($k_{R\text{-}Ph}/k_{Ph}$) vs. σ^+ values; (b) log($k_{R\text{-}Ph}/k_{Ph}$) vs. $\sigma^\bullet$ values; (c) log(d.r.) vs. σ^+ values; (d) log(e.r.) vs. σ^+ values.

The results suggest that reactivity of the homocoupling is governed by radical stabilizing ability. Through the course of the competition experiments, we found an interesting trend in stereoselectivity for the 1,4-dialdehyde products (d.r. relative to 1); MeO **3 c**: 5.0 ± 0.4 (96% *ee*); MeS **3 e**: 3.7 ± 0.7 (94% *ee*); Me **3 f**: 2.9 ± 0.6 (94% *ee*); H **3 i**: 1.5 ± 0.3 (66% *ee*); Br **3 g**: 1.6 ± 0.3 (32% *ee*); CF_3 **3 h**: 1.15 ± 0.06 (6% *ee*). The electron-rich 1,4-dialdehydes **3 c**,**e**,**f** were obtained with high diastereomeric ratios[22] and enantiomeric excesses, whereas 1,4-dialdehyde **3 h** bearing an electron-withdrawing substituent resulted in poor stereoselectivity. The reactivity correlates in a linear fashion with $\sigma^\bullet$ values, which are relative to radical stabilizing ability, whereas the logarithm of diastereomeric and enantiomeric ratios correlate linearly with σ^+ values (Figure 1 c,d).[23] These systems are mechanistically complex. The data suggest that with increasing electron-donating ability of the substituent, the energetic profile between the pathways distinguishing the two enantiomers must favor the experimentally obtained major product (*R*,*R*). This complexity might originate from the presence of an intermediate bearing both radical and cationic character.

Calculated IPs and linear free energy analysis support the claim that the homocoupling of α-branched aldehydes occurs via a radical cationic intermediate. Additionally, calculated energy barriers, if located, could provide further evidence for the proposed reaction pathway. It should be noted that potential energy profiles of radical species can be challenging because they often proceed on high-energy surfaces with shallow minima.[24]

DFT (Gaussian 09)[25] was used to calculate transition-state structures (TSSs) for the *para*-substituted 2-phenyl propanals **1 c**,**f**,**g**,**h**,**i** employing the unrestricted-ωB97X-D[26] functional with a 6–31 + G(d,p) basis set and the SMD solvent continuum model (see the Supporting Information for details).[27] DFT,

which is known to struggle with calculation of absolute barriers, can be quite useful in predicting trends. Unfortunately, all attempts at effectively modeling the trend in our relative rate ratios have been unsuccessful. Overall, it was found that **1 h** bearing a trifluoromethyl substituent had the highest reactivity barrier and **1 f** with a methyl substituent had the lowest barrier. Conformational analysis revealed that small changes in geometry led to significant energy differences in TSSs and intermediates, unfortunately not improving the correlation to experimental data. The relative rates account for the complete reaction conditions (e.g., heterogeneity, solvated silver species, full catalyst species, etc.), which necessarily affect the energetic profile, and these factors are not modeled by the DFT calculations. The predicted barriers, though not representative of the absolute barriers of this reaction, indicate that it is more energetically favorable for the homocoupling reaction to occur rather than for the second oxidation leading to **I**″ to take place (Scheme 2).

Conclusions

A novel strategy for the direct enantioselective oxidative homocoupling of α-branched aldehydes has been developed yielding succinic 1,4-dialdehydes. These products have been transformed into synthetically valuable chiral pyrrolidines. Calculated IPs in addition to competition experiments used to construct Hammett plots support that the homocoupling proceeds through a radical cation intermediate. Based on the mechanistic analysis, the reactivity is governed by radical character ($\sigma^{\bullet}$), whereas the diastereo- and enantioselectivities are influenced by cationic character (σ^{+}).

Acknowledgements

This work was made possible by grants from Carlsberg Foundation's 'Semper Ardens' programme, FNU, Aarhus University and DNRF. V.C. acknowledges the Alma Mater Studiorum-University of Bologna for financial support.

Conflict of interest

The authors declare no conflict of interest.

Keywords: density functional calculations · Hammett analysis · organocatalysis · oxidative coupling of aldehydes · pyrrolidines

[1] a) M. W. Rathke, A. Lindert, *J. Am. Chem. Soc.* **1971**, *93*, 4605; b) M. Schmittel, A. Burghart, W. Malisch, J. Reising, R. Sollner, *J. Org. Chem.* **1998**, *63*, 396; c) P. S. Baran, M. P. DeMartino, *Angew. Chem. Int. Ed.* **2006**, *45*, 7083; *Angew. Chem.* **2006**, *118*, 7241; d) H.-Q. Do, H. Tran-Vu, O. Daugulis, *Organometallics* **2012**, *31*, 7816; e) M. D. Clift, C. N. Taylor, R. J. Thomson, *Org. Lett.* **2007**, *9*, 4667; f) Y. Kohno, K. Narasaka, *Bull. Chem. Soc. Jpn.* **1995**, *68*, 322; g) For relevant review, see: F. Guo, M. D. Clift, R. J. Thomson, *Eur. J. Org. Chem.* **2012**, 4881.

[2] M. P. DeMartino, K. Chen, P. S. Baran, *J. Am. Chem. Soc.* **2008**, *130*, 11546.

[3] E. E. Robinson, R. J. Thomson, *J. Am. Chem. Soc.* **2018**, *140*, 1956.

[4] B. M. Casey, R. A. Flowers II, *J. Am. Chem. Soc.* **2011**, *133*, 11492.

[5] T. Amaya, Y. Maegawa, T. Masuda, Y. Osafune, T. Hirao, *J. Am. Chem. Soc.* **2015**, *137*, 10072.

[6] a) *Comprehensive Enantioselective Organocatalysis: Catalysts, Reactions, and Applications* (Ed. P. I. Dalko), Wiley-VCH, Weinheim, **2013**; b) B. Donslund, T. K. Johansen, P. H. Poulsen, K. S. Halskov, K. A. Jørgensen, *Angew. Chem. Int. Ed.* **2015**, *54*, 13860; *Angew. Chem.* **2015**, *127*, 14066; c) T. D. Beeson, A. Mastracchio, J.-B. Hong, K. Ashton, D. W. C. MacMillan, *Science* **2007**, *316*, 582.

[7] H.-Y. Jang, J.-B. Hong, D. W. C. MacMillan, *J. Am. Chem. Soc.* **2007**, *129*, 7004.

[8] a) J. J. Murphy, D. Bastida, S. Paria, M. Fagnoni, P. Melchiorre, *Nature* **2016**, *532*, 218; b) L. Ye, Q.-S. Gu, Y. Tian, X. Meng, G.-C. Chen, X.-Y. Liu, *Nat. Commun.* **2018**, *9*, 227.

[9] L. Næsborg, V. Corti, L. A. Leth, P. H. Poulsen, K. A. Jørgensen, *Angew. Chem. Int. Ed.* **2018**, *57*, 1606; *Angew. Chem.* **2018**, *130*, 1622.

[10] S. Manna, A. P. Antonchick, *Angew. Chem. Int. Ed.* **2016**, *55*, 5290; *Angew. Chem.* **2016**, *128*, 5376.

[11] M. Madesclaire, *Tetrahedron* **1986**, *42*, 5459.

[12] a) S. Cicchi, G. Ghini, L. Lascialfari, A. Brandi, F. Betti, D. Berti, S. Ferrati, P. Baglioni, *Chem. Commun.* **2007**, 1424; b) B. S. Donslund, A. Monleón, J. Larsen, L. Ibsen, K. A. Jørgensen, *Chem. Commun.* **2015**, *51*, 13666; c) M. Shi, Y. Satoh, T. Makihara, Y. Masaki, *Tetrahedron: Asymmetry* **1995**, *6*, 2109.

[13] E. Vitaku, D. T. Smith, J. T. Njardarson, *J. Med. Chem.* **2014**, *57*, 10257.

[14] K. Müller, F. Previdoli, H. Desilvestrio, *Helv. Chim. Acta* **1981**, *64*, 2497.

[15] M.-H. Le Tadic-Biadatti, M. Newcomb, *J. Chem. Soc. Perkin Trans. 2* **1996**, 1467.

[16] J. J. Devery III, J. C. Conrad, D. W. C. MacMillan, R. A. Flowers II, *Angew. Chem. Int. Ed.* **2010**, *49*, 6106; *Angew. Chem.* **2010**, *122*, 6242.

[17] R. J. Mullins, A. Vedernikov, R. Viswanathan, *J. Chem. Educ.* **2004**, *81*, 1357.

[18] E. V. Anslyn, D. A. Dougherty, *Modern Physical Organic Chemistry*, University Science Sausalito, CA, **2006**.

[19] F. A. Carey, R. J. Sundberg, *Advanced Organic Chemistry Part A: Structure and Mechanisms*. Springer, New York, **2007**.

[20] a) H. C. Brown, Y. Okamoto, *J. Am. Chem. Soc.* **1958**, *80*, 4979; b) C. G. Swain, E. C. Lupton, Jr., *J. Am. Chem. Soc.* **1968**, *90*, 4328.

[21] X. Creary, M. E. Mehrsheikh-Mohammadi, S. McDonald, *J. Org. Chem.* **1987**, *52*, 3254.

[22] The diastereomeric ratios are slightly different from those provided in Table 1; this difference is due to that the ratios in Table 1 are obtained after flash column chromatography.

[23] a) A. E. Wendlandt, P. Vangal, E. N. Jacobsen, *Nature* **2018**, *556*, 447; b) S. E. Shockley, J. C. Holder, B. M. Stoltz, *Org. Lett.* **2014**, *16*, 6362.

[24] N. J. Saettel, J. Oxgaard, O. Wiest, *Eur. J. Org. Chem.* **2001**, 1429.

[25] Gaussian 09, Revision B.01, M. J. Frisch, G. W. Trucks, H. B. Schlegel, G. E. Scuseria, M. A. Robb, J. R. Cheeseman, G. Scalmani, V. Barone, B. Mennucci, G. A. Petersson, H. Nakatsuji, M. Caricato, X. Li, H. P. Hratchian, A. F. Izmaylov, J. Bloino, G. Zheng, J. L. Sonnenberg, M. Hada, M. Ehara, K. Toyota, R. Fukuda, J. Hasegawa, M. Ishida, T. Nakajima, Y. Honda, O. Kitao, H. Nakai, T. Vreven, J. A. Montgomery, Jr., J. E. Peralta, F. Ogliaro, M. Bearpark, J. J. Heyd, E. Brothers, K. N. Kudin, V. N. Staroverov, R. Kobayashi, J. Normand, K. Raghavachari, A. Rendell, J. C. Burant, S. S. Iyengar, J. Tomasi, M. Cossi, N. Rega, J. M. Millam, M. Klene, J. E. Knox, J. B. Cross, V. Bakken, C. Adamo, J. Jaramillo, R. Gomperts, R. E. Stratmann, O. Yazyev, A. J. Austin, R. Cammi, C. Pomelli, J. W. Ochterski, R. L. Martin, K. Morokuma, V. G. Zakrzewski, G. A. Voth, P. Salvador, J. J. Dannenberg, S. Dapprich, A. D. Daniels, Ö. Farkas, J. B. Foresman, J. V. Ortiz, J. Cioslowski, D. J. Fox, Gaussian, Inc., Wallingford CT, **2009**.

[26] a) J.-D. Chai, M. Head-Gordon, *J. Chem. Phys.* **2008**, *128*, 084106–084101; b) J.-D. Chai, M. Head-Gordon, *Phys. Chem. Chem. Phys.* **2008**, *10*, 6615; c) M. Li, Y. Sang, X.-S. Xue, J.-P. Cheng, *Org. Chem.* **2018**, *83*, 3333.

[27] A. V. Manerich, C. J. Cramer, D. G. Truhlar, *J. Phys. Chem. B* **2009**, *113*, 6378.

Manuscript received: July 9, 2018

Accepted manuscript online: July 10, 2018

Version of record online: September 10, 2018